

A Practical Model for Realistic Butterfly Flight Simulation

QIANG CHEN, Jiangxi University of Finance and Economics, China

TINGSONG LU, East China Jiaotong University, China

YANG TONG, East China Jiaotong University, China

GUOLIANG LUO, East China Jiaotong University, China

XIAOGANG JIN, State Key Lab of CAD&CG, Zhejiang University, China

ZHIGANG DENG*, University of Houston, USA

As one of ubiquitous insects on the earth, butterflies are also widely-known for inspiring thrill resonance with their elegant and peculiar flights. However, realistically modeling and simulating butterfly flights, in particular, for real-time graphics and animation applications, remains an under-explored problem. In this paper we propose an efficient and practical model to simulate butterfly flights. Specifically, we first model a butterfly with parametric maneuvering functions, including wing-abdomen interaction. Then, we simulate dynamic maneuvering control of the butterfly through our force-based model that includes both the aerodynamics force and the vortex force. Through many simulation experiments and comparisons, we demonstrate that our method can efficiently simulate realistic butterfly flight motions in various real-world settings.

CCS Concepts: • Computing methodologies → Procedural animation.

Additional Key Words and Phrases: Computer animation, Butterfly animation, Aerodynamics, Maneuvering control.

ACM Reference Format:

Qiang Chen, Tingsong Lu, Yang Tong, Guoliang Luo, Xiaogang Jin, and Zhigang Deng*. 2022. A Practical Model for Realistic Butterfly Flight Simulation. *ACM Trans. Graph.* 1, 1 (January 2022), 12 pages. <https://doi.org/10.1145/nnnnnnnnnnnnnn>

1 INTRODUCTION

Realistic modeling and simulation of living things can find numerous potential applications, including, but not limited to, entertainment, virtual worlds, simulation, education, behavior analysis, and so on. In recent years, various efforts have been attempted to model and animate a variety of living things, include snakes [Miller 1988], fishes [Hwang et al. 2019; Meng et al. 2018], birds [Ju et al. 2013; Wu and Popović 2003], insects [Wang et al. 2014, 2015], ants [Xiang et al. 2019], etc.

Authors' addresses: Qiang Chen, Jiangxi University of Finance and Economics, 168 East Shuanggang Rd, Nanchang, Jiangxi, 330013, China; Tingsong Lu, East China Jiaotong University, 808 East Shuanggang Rd, Nanchang, Jiangxi, 330013, China; Yang Tong, East China Jiaotong University, 808 East Shuanggang Rd, Nanchang, Jiangxi, 330013, China; Guoliang Luo, East China Jiaotong University, 808 East Shuanggang Rd, Nanchang, Jiangxi, 330013, China; Xiaogang Jin, State Key Lab of CAD&CG, Zhejiang University, 866 Yuhangtang Rd, Hangzhou, Zhejiang, 310058, China; Zhigang Deng*, University of Houston, 4800 Calhoun Rd, Houston, Texas, USA, 77204.

* The Corresponding Author's Email: zdeng4@central.uh.edu.

Permission to make digital or hard copies of all or part of this work for personal or classroom use is granted without fee provided that copies are not made or distributed for profit or commercial advantage and that copies bear this notice and the full citation on the first page. Copyrights for components of this work owned by others than ACM must be honored. Abstracting with credit is permitted. To copy otherwise, or republish, to post on servers or to redistribute to lists, requires prior specific permission and/or a fee. Request permissions from permissions@acm.org.

© 2022 Association for Computing Machinery.

0730-0301/2022/1-ART \$15.00

<https://doi.org/10.1145/nnnnnnnnnnnnnn>

As one of the ubiquitous insects on the earth, butterflies are also widely-known for inspiring thrill resonance with their elegant and peculiar flights. Some previous efforts have been done to quantify and model butterfly flights. For example, researchers studied the principles of butterfly flights through aerodynamics theories, including the unsteady theory that integrates the Computational Fluid Dynamic (CFD) algorithms [Yokoyama et al. 2013]. Also, researchers developed experimentally-grounded methods that employ wind tunnel measurements to gauge the aerodynamics for modeling butterflies [Ortega Ancel et al. 2017; Srygley and Thomas 2002]. However, realistically modeling and simulating butterfly flights, in particular, for real-time graphics and animation applications, remains an under-explored problem, due to the following main reasons: i) Experiment-based methods have difficulty to acquire the full trajectories and natural body motions of real-world butterflies; ii) CFD-based methods are impracticable to simulate the motion of butterflies in real-time due to their high computational cost; and iii) unlike many flying insects, a butterfly with charming wings and abdomen can normally fly with small flapping frequencies [Huang and Sun 2012; Sridhar et al. 2016]. Therefore, without taking into account wing-body interaction, it is impossible to simulate the natural and dynamic flight behavior of butterflies in various real-world settings.

In this paper we focus on the efficient simulation of realistic butterfly flights in real-world settings, taking wing-body interaction into consideration. Specifically, we first model a butterfly with parametric maneuvering functions, including wing-abdomen interaction. Then, we simulate dynamic maneuvering control of the butterfly through our force model that includes both the aerodynamics force and the vortex force. Through various simulation experiments and comparisons, we demonstrate that our method can simulate realistic butterfly flight motions in various real-world settings.

The main contributions of this work can be summarized as follows:

- We propose a first-of-its-kind, practical model to simulate butterfly flights with maneuvering functions, which is particularly suitable for real-time graphics and animation applications.
- We introduce a novel force model to simulate the dynamic flight motion of butterflies through both efficient maneuvering control and wing-body interaction modeling.

The remainder of this paper is organized as follows. In Section 2, we review the related work on the simulation of flying creatures. Then, we present our schema in Section 3. In the following sections, the details of butterfly modeling and parameters are presented in

Section 4; the forces for butterfly flights are explained in Section 5, with detailed descriptions on aerodynamics forces (Section 5.1) and vortex forces (Section 5.2); in Section 6, we describe the details of dynamic maneuvering control. Finally, we present our results in Section 7 and discussion and conclusion in Section 8.

2 RELATED WORK

In this section, we briefly review recent related works on the simulation of flying creatures. In general, among the existing works on flying creature simulation, we can roughly divide them into individual flying creature simulations and swarm simulations.

Flying Creature Simulations. Many physically-based modeling and simulation approaches were proposed for various flying species, including birds [Ju et al. 2013; Ren et al. 2018; Wu and Popović 2003; Zhu et al. 2006], dragonflies [Isogai et al. 2004; Young et al. 2008], bats [Pivkin et al. 2005], etc. Specifically, Wu et al. [2003] apply aerodynamics to animate the bird's wing flapping, and they optimize the maneuvering parameters of both the wings and feathers through an offline method. To increase the efficiency and visual quality, Ju et al. [2013] also use the aerodynamics theory to animate realistic bird flights. They first use an advanced experimental measurement equipment to capture a real bird's motion and then use the captured data to optimize flight simulations.

In the field of bio-mechanical simulation, many experiment-based methods [Bode-Oke and Dong 2020; Naranjo 2019; Senda et al. 2012; Slegers et al. 2017; Wang 2005] were proposed for the analysis and simulation of flying insects. For example, Senda et al. [2012] use a wind tunnel to measure the butterfly's aerodynamics forces, which are then used to simulate the wings' flapping. Bode-Oke et al. [2020] simulate the body motion of a monarch butterfly to understand the backward flight kinematics based on the CFD solver. It is noteworthy that although the CFD solver can simulate more accurate wing aerodynamics forces, their method involves heavy computation of the Navier-Stokes equation, which is impracticable for real-time butterfly simulation applications. Dickson et al. [2006] simulate a flying insect as a rigid body. Later, along this line, a few methods were proposed to simulate the butterfly as a rigid body while integrating the abdomen's inertia and moment [Sridhar et al. 2020; Wilson and Albertani 2014]. However, because these methods primarily focus on the wings and abdomen's oscillations, they generally fall short of generating realistic flight trajectories.

Compared to the existing aerodynamics-based methods (e.g., [Bode-Oke and Dong 2020; Senda et al. 2012]), the main distinctions of our approach include: (i) Instead of heavily depending on the computationally expensive CFD solver, our approach directly connects simplified aerodynamic forces with maneuvering functions of the butterfly. (ii) To simulate accurate butterfly body deformation during flights, besides introducing a hierarchical skeleton, our approach also introduces a new vortex force to simulate the wake influence of wing flapping and generate plausible butterfly motion.

Swarm Simulations. The seminal Boids model [Reynolds 1987] is a simple yet effective technique for animating flocks. However, it does not support physical forces for realistic simulation. By contrast, the bio-inspired flying insect simulation [Wang et al. 2015], mainly

based on the three-space model [Couzin et al. 2002], can generate more realistic noisy motions of flying insects. To animate the inherent dynamics of flying insects, Wang et al. [2014] apply a curl-noise field to compute collision-free trajectories for flying insects. In addition, chaotic behavior of flying insects was also extended to generate special effect animation [Chen et al. 2019]. With the recent advances of computer vision techniques, data-driven methods for generating visually-plausible animations of flying insects have become increasingly applicable. However, the above swarm simulation methods are focused on macro-level motion of the swarm, that is, generating trajectories of insects in the swarm. For the micro-level motion of individual insects, they just often use cycle-frames (i.e., loop playing of a pre-created sequence) as the individual motion presentation.

3 OUR APPROACH

Our approach consists of three main inter-connected modules: butterfly modeling, forces computation, and maneuvering control. We give a brief overview on each module below. Figure 1 illustrates the pipeline of our approach. For the sake of clarity, Table 1 lists all the notations defined in this paper as well as their descriptions.

Butterfly modeling. We create a butterfly mesh model rigged with a hierarchical skeleton, which is used to animate and control the motion of the butterfly. Moreover, we also define a set of parametric maneuvering functions to control the wing-abdomen interaction of the butterfly.

Forces computation. Besides a simplified aerodynamics force for wing deformation, we also introduce a vortex force to simulate the wake influence of the wings' flapping. Based on the defined force model, we then control butterfly motion by integrating with attraction targets.

Maneuvering control. We introduce an effective maneuvering control method through body motion decoupling. Based on the computed aerodynamics forces, vortex forces and attraction from the target, we obtain the velocity of the butterfly. Then, based on the velocity, we further update its body deformation and position. By using a sliding window algorithm, we continuously update maneuvering control parameters to produce smooth and realistic butterfly flight animations.

4 BUTTERFLY MODELING

Without the loss of generality, in this work we construct 3D models for two butterfly species, namely, swallowtail butterfly (*Pachliopta aristolochiae*) and monarch butterfly (*Danaus plexippus*), due to their wide existence on the earth. A swallowtail butterfly flies through flapping the fore-wings, but a monarch butterfly flies with a trivial difference of the flapping angles between the fore-wings and the hind-wings. The detailed body descriptions of the swallowtail and monarch butterflies, including size, mass, chord, and the wing's area, can be referred to existing literature and public databases [Sridhar et al. 2016; Tanaka and Shimoyama 2010], which are summarized in Table 2. In this work, the constructed monarch 3D model has 11,814 vertices and 23,334 triangles, and the swallowtail 3D model has 16,596 vertices and 16,594 triangles. In addition, the numbers of the triangles of the wings are 4,132 (swallow-tail butterfly) and 2,096 (monarch butterfly), respectively. Each of the constructed

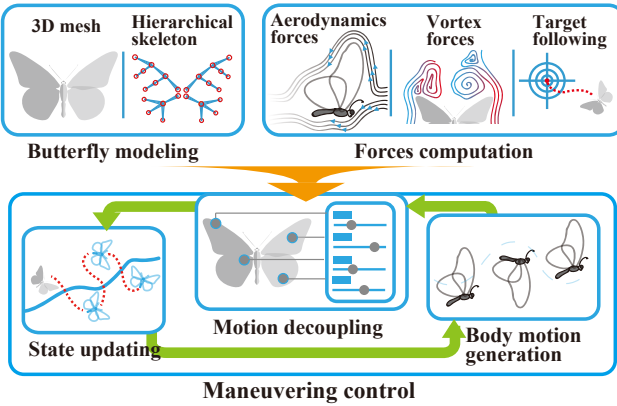


Fig. 1. The pipeline of our approach. First, we construct a butterfly mesh model rigged with a hierarchical skeleton. Then, based on the aerodynamics force and the vortex force, we compute the inherent noisy behavior and rapidly-adjusted body motion. Finally, we use an efficient maneuvering control method through motion decoupling to generate butterfly body motion and trajectories.

Table 1. The used notations and their descriptions in this paper

Notation	Description
θ_β	pitch angle of the thorax
θ_γ	flapping angle of the wings
θ_ζ	feathering angle
θ_ψ	sweeping angle
θ_ϕ	rotation angle of the abdomen
φ_a	amplitude
f	frequency
φ_p	phase angle
φ_m	the mean angle
R_f	range of the frequency
$ u^{max} $	max speed of butterfly
R_{θ_a}	range of the amplitude
\mathbf{u}	velocity of the butterfly
\mathbf{p}	mass center of the thorax
\mathbf{a}	acceleration of the butterfly
α	angle of attack
ρ	air density
A_i	the area of the i -th polygon
V	the air velocity over the wing's surface

butterfly mesh models consists of five parts: head, thorax, abdomen, fore-wings, and hind-wings, as illustrated in Figure 2.

Based on the Unity Dynamic Bone model [Will 2020], we drive the movement of the butterfly models through a pre-created hierarchical skeleton. Specifically, the thorax is the root that links the fore-wings, the hind-wings, and the abdomen through the body longitude axis. The skeleton of the butterfly model is depicted in Figure 3. Considering the deformation of real-world butterfly wings is mainly triggered by the leading-edge of the wings (especially

Table 2. The wing area and mass of the body parts of the two selected butterfly species

Name	wing area ($10^{-4} m^2$)	Body Mass (g)
Monarch	26	0.428
Swallowtail butterfly	28	0.34

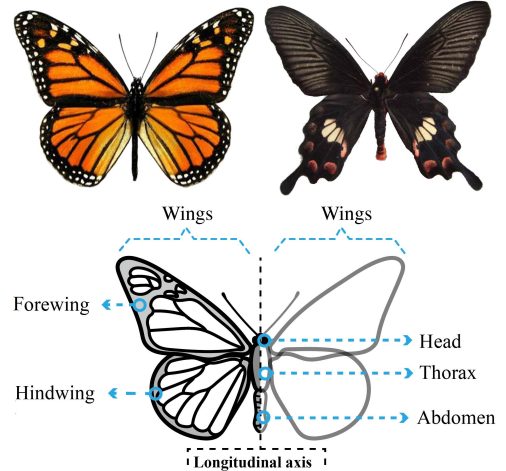


Fig. 2. Schematic illustration of a butterfly's anatomical structure. The top-left is a monarch butterfly, and the top-right is a swallowtail butterfly.

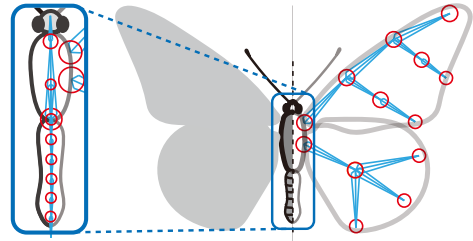


Fig. 3. Illustration of the hierarchical skeleton rigged with a butterfly model in this work.

the fore-wings) during flapping, we rig the virtual wing skeleton along the leading-edge from the root to the wing-tip. In our work, we use two parameters, i.e., elasticity and stiffness, to simulate the deformation of the wings and abdomen. Besides the gravity force, the aerodynamics force (refer to Section 5.1) as a global force is also applied to the root joint when the wings are flapping. Finally, based on the applied forces at each frame, the Dynamic Bone model [Will 2020] can further compute the positions and angles of the skeleton joints.

Generally, the bilateral wings of the butterfly perform flapping with synchronous frequencies [Dudley 2002]. As such, in this work we also treat the butterfly with synchronous frequencies of bilateral wings' flapping motion.

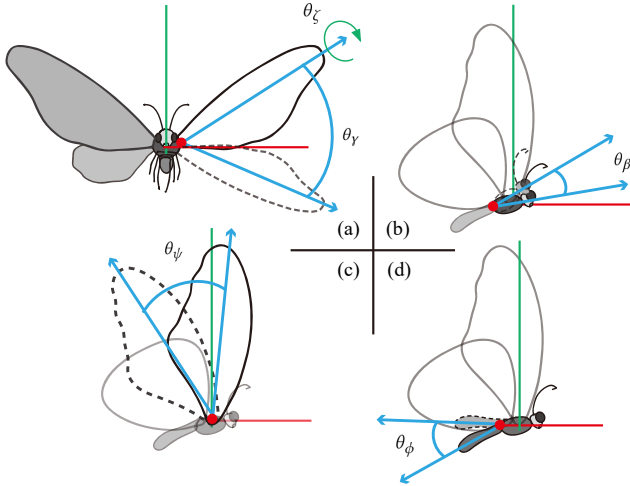


Fig. 4. The abdomen's rotation angle θ_ϕ and the thorax pitch angle θ_β are illustrated in (d) and (b), respectively. Using the fore-wing as an example, the fore-wing's flap angle θ_γ and feather angle θ_ζ are illustrated in (a), and its sweep angle θ_ψ is illustrated in (c).

4.1 Maneuvering Parameters and Functions

The joint-linked wings of the butterfly flap with a limited range of frequencies and phases. Moreover, according to the findings in [Huang and Sun 2012; Sridhar et al. 2016], a butterfly deforms its abdomen to counteract with wing flapping while flying forward or climbing up/down. To simulate these phenomena, we design the following parameters to model the butterfly's maneuvering.

Parameters for thorax. The thorax coordinates the wings' flapping through undulating during flights [Kang et al. 2018; Yokoyama et al. 2013]. In our work, we treat the thorax as the root of the butterfly with one Degree of Freedom (DOF). The controllable parameters for the thorax is denoted as the pitch angle θ_β (refer to Fig. 4(b)).

Parameters for wings. For simplicity, we take the bilateral wings' flapping with synchronous frequencies. Furthermore, in our butterfly model, each fore-wing has 3-DOFs to rotate. Each hind-wing only has 1-DOF for flapping due to its less significant contribution to the flight [Jantzen and Eisner 2008]. The wing-beat parameters include the flapping angle θ_γ for both the fore-wings and the hind-wings (Fig. 4(a)), the feathering angle θ_ζ for the fore-wings (Fig. 4(a)), and the sweeping angle θ_ψ for the fore-wings (Fig. 4(c)).

Parameters for abdomen. The abdomen of the butterfly may visibly rotate along the body longitude axis with the opposite phase to the wings' flapping while it plans to hover or climb [Sridhar et al. 2020]. We assign the abdomen with 1 DOF to rotate along the body longitudinal axis. θ_ϕ is defined as the abdomen's rotation angle (Fig. 4(d)). To this end, we define χ as the set of the above five maneuvering angle parameters: $\chi = \{\theta_\beta, \theta_\gamma, \theta_\zeta, \theta_\psi, \theta_\phi\}$.

To effectively simulate body oscillations, in our work we simplify body undulation as periodical motion. In addition, for the purpose of smooth animation generation, we let the wing flapping motion (wing-beat) during a full cycle start from the highest position to the lowest and then back to the highest position. Let t_0 and t_1 denote the

starting and ending time of a flapping cycle, respectively. Then, the maneuvering angles $\{\theta_\beta, \theta_\gamma, \theta_\zeta, \theta_\psi, \theta_\phi\}$ at a given time t between t_0 and t_1 can be determined through maneuvering functions, described in Equation (1). Figure 5 shows the phases shifts of the five maneuvering angles of the butterfly during a flapping cycle (including the up-stroke and down-stroke).

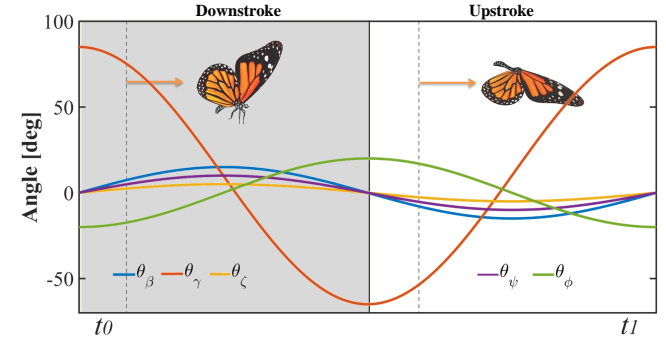


Fig. 5. The phase shifts of the maneuvering angles of the butterfly during one wing flapping cycle (including the up-stroke and the down-stroke of wing flapping). t_0 to t_1 on the X axis denotes the time from the beginning of the down-stroke to the end of the upstroke of wing flapping.

Inspired by the periodic maneuvering design in [Wilson and Albertani 2014; Wu and Popović 2003], we compute the five maneuvering angles $\chi = \{\theta_*\}$ as follows:

$$\theta_*(\varphi_a^*(\mathbf{u}), f^*(\mathbf{u}), \varphi_p^*, \varphi_m^*, t) = \varphi_a^*(\mathbf{u}) \cos(2\pi f^*(\mathbf{u})t + \varphi_p^*) + \varphi_m^*. \quad \text{where } * \in \{\beta, \gamma, \zeta, \psi, \phi\} \quad (1)$$

Equation (1) is based on the time t and other internal control parameters including: amplitude $\varphi_a^*(\mathbf{u})$, which is a function of the butterfly velocity \mathbf{u} ; frequency $f^*(\mathbf{u})$, which is also a function of the butterfly velocity \mathbf{u} ; the mean value of the angle φ_m^* ; and the phase angle φ_p^* . $\varphi_a^*(\mathbf{u})$ and $f^*(\mathbf{u})$ can be dynamically adjusted based on the velocity of the butterfly, but the adjustment only can be done across different flapping cycles. Because in our work we assume the butterfly keeps the frequency parameter f and the amplitude parameter φ_a unchanged within one flapping cycle. The value of φ_p^* is 0 when Equation (1) is used for computing the wing maneuvering parameters (that is, for computing θ_γ , θ_ζ , and θ_ψ), while it is -180° when Equation (1) is used for computing the abdomen maneuvering parameter θ_ϕ , since the abdomen has the opposite phase to the wings' flapping while the butterfly plans to hover, climb up, or move down [Sridhar et al. 2020]. Furthermore, φ_p^* is -90° when Equation (1) is used for computing the thorax's maneuvering parameter θ_β . φ_m^* keeps the same across different flapping cycles.

Since the frequency $f^*(\mathbf{u})$ in Equations (1) is assumed to be fixed within one flapping cycle, we empirically design and compute f^* using the butterfly velocity at t_0 as follows:

$$f^*(\mathbf{u}(t_0)) = R_f^* \frac{1}{(1 + e^{-16(|\mathbf{u}(t_0)|/|\mathbf{u}^{max}| - 0.5)})}, * \in \{\beta, \gamma, \zeta, \psi, \phi\} \quad (2)$$

Table 3. Values of some parameters used in our experiments

Angle	Parameter Value			
	R_{f_a} (Hz)	R_{θ_a} (°)	φ_p (°)	φ_m (°)
θ_β	0~3	0~30	-90	0
θ_γ	0~11	0~150	0	10
θ_ζ		0~10	-90	0
θ_ψ		0~20	-90	0
θ_ϕ		0~35	-180	-10

where R_f^* is the frequency range of the specific maneuvering angle θ_* , $|\mathbf{u}^{max}|$ is the maximum flying speed of the butterfly, and $\mathbf{u}(t_0)$ is the butterfly velocity at time t_0 .

Analogously, we empirically design and compute the amplitude φ_a^* of a maneuvering angle as follows:

$$\varphi_a^*(\mathbf{u}(t_0)) = R_{\theta_a}^* \frac{1}{(1 + e^{-16(|\mathbf{u}(t_0)|/|\mathbf{u}^{max}| - 0.5)})}, * \in \{\beta, \gamma, \zeta, \psi, \phi\} \quad (3)$$

where $R_{\theta_a}^*$ denotes the amplitude range of the specific maneuvering angle θ_* .

In this work, we obtain the maximum flying speed, and the ranges of both the frequencies and amplitudes of butterflies from existing bio-mechanical literature [Kang et al. 2018; Sridhar et al. 2016], which are used in the above Equations (2) and (3). Specific values of all the important parameters (including φ_p^* , φ_m^* , $R_{\theta_a}^*$, and R_f^*) used in this work are summarized in Table 3. Note that the parameter values listed in Table 3 may not be perfectly consistent with those of a real butterfly. For example, the flapping frequency of a real monarch butterfly is typically confined between 9 and 11 Hz [Kang et al. 2018], but in our work we set the range of the flapping frequency from 0 and 11 Hz. The extra flexibility of the flapping frequency allows us to simulate various butterfly gliding behaviors in virtual worlds.

5 FORCES COMPUTATION

During simulations, the instantaneous forces applied onto the butterfly consist of a simplified aerodynamics force on the wings (Section 5.1) and a vortex force on the thorax (Section 5.2).

5.1 Simplified Aerodynamics Force

The aerodynamics forces originate from the wings' up-stroke and down-stroke for flying creatures. A butterfly can obtain a lift force from its wings' flapping, and a drag force is caused by air friction. We compute the simplified aerodynamics forces acting on the i -th polygon of the butterfly model based on the quasi-state theory [Ellington 1984a]. Thus, the aerodynamics forces can be computed as follows:

$$\mathbf{F}_{i,lift} = \frac{1}{2} \rho A_i |\mathbf{V}|^2 C_l(\alpha) \quad \text{and} \quad \mathbf{F}_{i,drag} = \frac{1}{2} \rho A_i |\mathbf{V}|^2 C_d(\alpha), \quad (4)$$

where ρ is the air density, A_i is the area of the i -th polygon, \mathbf{V} is the air velocity over the wing's surface. $C_l(\alpha)$ and $C_d(\alpha)$ are the coefficients of the lift force $\mathbf{F}_{i,lift}$ and the drag force $\mathbf{F}_{i,drag}$,

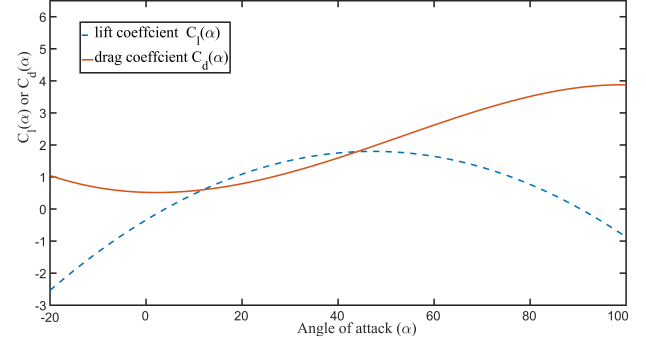


Fig. 6. Relation between the wing's local angle of attack α and the coefficients $C_l(\alpha)$ and $C_d(\alpha)$. The lift coefficient function (blue curve): $-0.0095953\alpha^2 + 0.090635\alpha - 0.34182$, and the drag coefficient function (red curve): $-0.0000079518\alpha^3 + 0.0011527\alpha^2 + 0.0063148\alpha + 0.51127$.

respectively. The coefficients $C_l(\alpha)$ and $C_d(\alpha)$ are determined by the wing's local angle of attack, α , which can be computed as follows:

$$\alpha = \arctan\left(\frac{|\mathbf{V}^n|}{|\mathbf{V}^t|}\right), \quad (5)$$

where \mathbf{V}^n and \mathbf{V}^t are the components of the air velocity along the normal of the wing surface and along the tangent direction (i.e., the vector of base-to-tip), respectively. Figure 6 plots the relation between the wing's local angle of attack α and the coefficients $C_l(\alpha)$ and $C_d(\alpha)$. To the best of our knowledge, there are not commonly-used Lift/Drag coefficients for butterflies because each kind of flying creatures may have different Lift/Drag coefficients. Based on our experiments, we propose empirical Lift/Drag coefficient functions for butterfly flight motion, as shown in Figure 6.

Let $\mathbf{F}_{i,j} = \mathbf{F}_{i,lift} + \mathbf{F}_{i,drag}$ be the resultant aerodynamics force acting on the i -th polygon of the j -th wing, then the instantaneous force \mathbf{F}_j acting on the skeleton from the j -th wing can be computed as follows:

$$\mathbf{F}_j = \sum_i \mathbf{F}_{i,j}. \quad (6)$$

5.2 Vortex Force

Many previous research studies confirmed that the leading edge of the wing triggers vortices and produces a vertical lift force for flying insects [Ellington 1984b; Srygley and Thomas 2002]. However, CFD-based methods that solve the Navier-Stokes equation for vortex simulations are computationally expensive. Furthermore, situations will become more complex if we want to analyze the influence when a dense swarm of flying insects aggregates in the air. In this work, we assume that the fast time-variation of vortices also influences the flight of a butterfly. Moreover, flying insects also present inherent noise behavior such as tight turn [Betts and Wootten 1988] and vortex-like motion [McInnes 2007].

To simulate the influence of the vortices and the inherent chaotic behavior, we compute an artificial force from a curl-noise field, which is a procedural approach proposed by Bridson et al. [2007] for fluid simulations. By integrating with the Perlin noise [Perlin 2002] to animate the inherent noise behaviors [Betts and Wootten 2002]

1988; McInnes 2007], we extend the curl-noise force into low-level simulations as a vortex force acting on the thorax while decoupling the body motion for the butterfly.

The vortex force can be computed as follows:

$$\mathbf{F}_{vor} = \nabla \times \left(\left(s_1 \left(\frac{\mathbf{p}}{gain_x} \right), s_2 \left(\frac{\mathbf{p}}{gain_y} \right), s_3 \left(\frac{\mathbf{p}}{gain_z} \right) \right) * \eta \right), \quad (7)$$

where \mathbf{F}_{vor} denotes the vortex force, \mathbf{p} is the gravity center of the body (thorax), s_1 , s_2 and s_3 are the values produced by the Perlin noise function with different noise seeds at \mathbf{p} , $gain$ and η are the parameters used to scale the noise grid density and the magnitude of the Perlin noise, respectively. The parameter $gain$ mainly influences the vortices' shapes: smaller gain values can lead to smaller vortices; and vice versa. The parameter η mainly influences the magnitude of the vortex force. In our experiments, we empirically set both $gain_x$ and $gain_z$ to 22.0, set $gain_y$ to 5.5, and set η to 3.66.

Note that the above artificial vortex force is used to real-time simulate the wake influence, although it may not be physically accurate. Based on our experiments, we found that when the computed vortex force was directly applied onto the wings, it could lead to excessive twisting on the wings due to both the potentially excessive amplitude and less predictable direction of the vortex force. Thus, we only apply the vortex force to the mass center of the thorax of the butterfly. In our approach, the wing flapping is not *directly* driven by the vortex force. Instead, the frequency and amplitude of wing flapping are computed based on the velocity (refer to Equation (2) and Equation (3)) that is dynamically changed by the composite force via acceleration. We will describe how we obtain the acceleration from the vortex force in the follow-up Section 6.

6 MANEUVERING CONTROL

In the wild, a real-world butterfly exhibits peculiar flying styles not only for inherently noisy trajectories but also for rapidly-adjusted body motion. It is non-trivial to generate both the inherently noisy trajectories and rapidly-adjusted body motion for flying butterflies simultaneously. To achieve this, we decouple the body motion while driving the butterfly by our force model.

6.1 Velocity Computation

To animate the realistic flying motion of the butterfly, we let the butterfly fly towards a given target (e.g., a virtual flower) or let the butterfly follow along a user-specified path. Thus, we can compute a preferred acceleration \mathbf{a}_{pre} from the given target or a set of user-specified key points that defines a path. However, the butterfly may not strictly hover above the target or follow along a pre-defined global path like a virtual bird in [Ju et al. 2013; Wu and Popović 2003]. Generally, the butterfly endeavors to arrive at a destination, with highly dynamic motion in the process. Further, the butterfly employs its vision to distinguish gender [Li et al. 2017] and sense the environment [Stewart et al. 2015]. Therefore, we design a vision-based algorithm to animate the chaotic motion of the butterfly while it is approaching an attraction target. Specifically, its preferred acceleration can be computed as follows:

$$\mathbf{a}_{pre} = R(d) \frac{1}{m} \frac{\mathbf{p} - \mathbf{q}_i}{|\mathbf{p} - \mathbf{q}_i|}, \quad (8)$$

where \mathbf{q}_i is the closest attraction point, \mathbf{p} is the gravity center of the butterfly body, m is the total mass of the butterfly, and $d = \min(1, |\mathbf{p} - \mathbf{q}_i|/L)$, L is the maximum sensory length in the field of view (FOV) of the butterfly. The butterfly would not be attracted when its distance to the target was larger than L . FOV acts as the instantaneous sensing space for the butterfly. L is empirically set to 4.5 in our experiments. Also, in Equation (8) we introduce a ramp function $R(d)$ to smoothly cool down its velocity when the butterfly approaches the target. Although different ramp functions could be used, in this work we define $R(d)$ as follows:

$$R(d) = \begin{cases} \frac{15}{8}d - \frac{10}{8}d^3 + \frac{3}{8}d^5, & d \leq 1; \\ 0, & \text{otherwise.} \end{cases} \quad (9)$$

Our approach drives the butterfly by using both the vortex force and the aerodynamics force, besides the gravity \mathbf{g} . Based on the Newton's Second Law, we compute the local acceleration \mathbf{a}_{loc} based on the resultant composite force as follows:

$$\mathbf{a}_{loc} = (\sum_{j=1}^4 \mathbf{F}_j + \mathbf{F}_{vor} + \mathbf{g})/m, \quad (10)$$

where $\sum_{j=1}^4 \mathbf{F}_j$ is the resultant aerodynamics force of all the four wings.

Finally, we can obtain the actual acceleration of the butterfly by summing up \mathbf{a}_{loc} and \mathbf{a}_{pre} . Let \mathbf{u}_{t-1} denote the velocity of the butterfly at the previous time step $t-1$, we can compute the velocity \mathbf{u}_t at the current time step t as follows:

$$\mathbf{u}_t = \mathbf{u}_{t-1} + (\mathbf{a}_{loc} + \mathbf{a}_{pre})\Delta_t. \quad (11)$$

6.2 Maneuvering Update

To generate dynamic motion of the butterfly, we may need to update the values of two internal control parameters, f and φ_a , across different flapping cycles. Recall in Section 4.1, we assume both f and φ_a keep fixed within one flapping cycle, but they can be adjusted before entering into the next cycle.

The drastic change of the frequency or amplitude does not help to save energy during the butterfly's flights [Dudley 1991]. Also, the persistent drastic change of the frequency and amplitude will lead to less smooth motion. As such, we need to smooth the values of both f and φ_a . Based on the sliding window algorithm, we use the values of f and φ_a in both previous flapping cycles and the current cycle to compute the parameter values at the next cycle, described below:

$$c_{n+1}^* = 0.5 \left(\sum_{i=\max(n-k,1)}^{n-1} w_i c_i^* \right) + 0.5 c_n^*, \text{ where } * \in \{f, \varphi_a\} \quad (12)$$

where c_n^* represent the value of the control parameter $*$ at the current flapping cycle n , which can be computed using the Equation (2) or Equation (3); c_{n+1}^* represents the value of the control parameter $*$ used at the next cycle $n+1$; $\sum w_i = 1$ and k is the size of the sliding window. In our experiments, k is empirically set to 10.

7 RESULTS AND EVALUATIONS

All of the animation results in this paper were obtained in the Unity engine. We used our approach to simulate the flights of butterflies



Fig. 7. A virtual swallow-tail butterfly automatically adjusts its body postures while flying along a global path as much as possible.



Fig. 8. Snapshots of an animated monarch butterfly flying along a given path. It automatically adjusts its body postures during the flight.

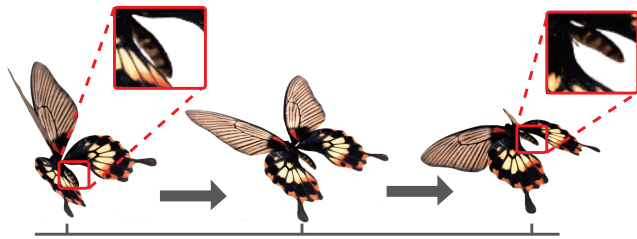


Fig. 9. The simulated wing-abdomen interaction during the flight of a swallow-tail butterfly. The magnified windows show the detailed deformation of the wings and abdomen.

in various scenarios and environments, which are reported in Section 7.1. The animation results by our approach can be found in the supplemental demo video.

7.1 Results

We simulated various butterfly flight scenarios, including flying along a user-specified path, interacting with wind, flying in the rain, butterfly chasing, aggregation, and traveling, which are described below. The aggregation and traveling experiments are mainly used to demonstrate that our approach can be straightforwardly extended for butterfly swarm simulations.

Flying along a user-specified path. A butterfly flying along a user-specified path is commonly seen in simulations or virtual environment. However, unlike birds, a butterfly may not be able to faithfully follow along a given path, but have inherently noisy, dynamics behavior in this process. As shown in Figure 7 and Figure 8, the body motion and fast undulating of the wings of the simulated butterfly by our approach can be observed, in particular, the wing-abdomen interaction can be clearly observed with a magnified view (refer to Figure 9).

Interacting with wind. Our model can also handle the influence of various external forces on the butterfly during flights, such as wind. Figure 10 shows the motion responses of a flying butterfly when influenced by two different types of winds. As shown in this figure (as well as the demo), the butterfly attempts to recover a stable flight whenever it is influenced by external forces. Also,

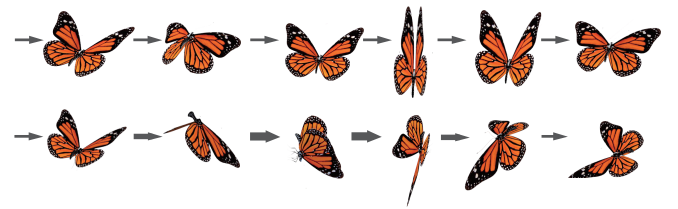


Fig. 10. Our method can simulate a flying butterfly under external force influence. The top row shows snapshots of the butterfly under the influence of a constant wind force. The bottom row shows snapshots of the butterfly under a varying wind force. The direction of the arrow in each snapshot represents the direction of the wind force at that moment, and its width visualizes the strength of the wind force.

an interesting spiral trajectory can be observed. When the wind disappears, the butterfly gradually recovers its normal flight state.



Fig. 11. Spirally falling motion can be observed when the butterfly is hit by the rain.

Flying in the rain. To test whether our approach can robustly handle the influence from other environmental factors, we simulated a butterfly flying in the rain. The rain was simulated as particles with varied masses and directions. A spirally falling motion can

be observed when the butterfly is hit by the rain, as shown in Figure 11. The animation result of this experiment is enclosed in the supplemental demo video.



Fig. 12. A snapshot of the simulated butterfly chasing scenario

Chasing. We also simulated a scenario where two virtual butterflies are chasing each other. As shown in Figure 12 (also refer to the demo video), the follower butterfly automatically adjusts its body postures to chase the leader butterfly during the process. It is noteworthy that the simulated butterflies in the chasing example are different butterfly species (i.e., different from the one in Figure 7). From the chasing example as well as additional comparisons (refer to Section 7.2), we demonstrate that our model can simulate the flight motion of a range of butterflies.

Aggregation. Our model can also be straightforwardly extended to real-time simulate a swarm of butterflies. In the real world, many butterfly species tend to aggregate for migration, such as monarch. Moreover, a swarm of butterflies can exhibit more visual effects for artists' creation. As shown in Figure 13, we animated more than 100 butterflies using our approach, achieving a real-time speed of 25 frames per second. The macro inherent-noise trajectories of densely aggregated butterflies can be observed. Meanwhile, the body motions of the butterflies were automatically computed according



Fig. 13. Our method can be extended to animate a virtual swarm of butterflies. As shown in this figure, butterflies in the swarm exhibit various wing-body motions during their flights.



Fig. 14. Butterfly aggregation and traveling results simulated by our approach. The top panel shows a snapshot of a recorded video of traveling monarch butterflies in the wild, while the bottom panel shows the simulation result by our approach.

to their flight states. Note that, in this experiment, we did not need to specify a path for each butterfly, since the force-driven butterflies fly with chaotic trajectories without collisions. In a sparse scene, generally collisions can be avoided thanks to the divergence-free curl field between any pair of butterflies.

Traveling. In addition, we used our approach to simulate a butterfly traveling scenario, as shown in the bottom of Figure 14. The simulated butterflies exhibit various dynamic motions such as floating during the traveling. In this experiment, we also directly compare our simulation result with the video footage of real butterflies' traveling (refer to the top of Figure 14). From the comparison, we can see the simulated virtual butterflies are realistic, and they demonstrate similar dynamic behaviors as those real butterflies in the wild.

Runtime statistics. We ran all the simulation experiments by our approach on an off-the-shelf PC with Intel(R) Core(TM) i7-7700 CPU, GeForce RTX 2070 GPU (8G), and 16GB memory. The simulation performances of our approach are reported in Table 4. Note that our current implementation is un-optimized and does not use any computational power of GPU, we believe the simulation efficiency of our approach can be significantly improved if GPU and code optimization were utilized.

Table 4. Runtime statistics of our experiments, including FPS (frames per second) and the computational time for two major components in our approach (the computation of aerodynamic force and the computation of vortex force). Here “*along path*” refers to the experiment “flying along a user-specified path” (Figure 9), “*with wind*” refers to the experiment “interacting with wind” (Figure 10), “*raining*” refers to the experiment “flying in the rain” (Figure 11), and “*direct compare*” refer to the experiment “direct comparison with a real butterfly” (Figure 15).

ID	experiment	# agents	FPS	Aero Force (ms)	Vortex Force
1	along path	1	60	0.41	0.08
2	with wind	1	60	0.46	0.08
3	raining	1	60	0.45	0.08
4	chasing	2	60	0.76	0.14
5	aggregation	100	25	33.69	6.99
6	traveling	200	15	50.56	13.78
7	direct compare	1	60	0.42	0.08

7.2 Comparisons

Due to the infeasibility to obtain ground-truth butterfly flight trajectories (e.g., lacking of such publicly shared data for scientific research), we were not able to validate our method through a direct comparison with ground-truth butterfly trajectory data. However, besides an ablation study, in this work we compared our approach with a baseline approach, and directly compared our result with a video footage of a flying butterfly in the real world, described below.

Ablation study. We conducted an ablation study to evaluate the contribution of the vortex force in our force model. In this study, we generated the butterfly animations using two conditions: the first was animated by our complete approach, and the second was animated by our approach but without the vortex force. As shown in the demo video, the simulated butterfly by our complete approach exhibits inherent-noisy trajectories and realistic wing-abdomen interaction; by contrast, the simulated butterfly without the vortex force loses the dynamics although it still can faithfully fly along a specified path.

Comparison with a baseline approach. In this comparison experiment, we chose the de facto cycle-frames animation as the baseline approach. The comparison result (refer to the supplemental demo video) demonstrates that our method can generate more realistic butterfly body motion, such as gliding and wing-abdomen interaction, than the baseline approach.

Direct comparison with a real butterfly. We also simulated the flying of a single virtual butterfly by directly comparing it with a real one in video. Specifically, we downloaded a butterfly video clip from YouTube.com and then randomly selected a segment of the video as the comparison example. According to the butterfly in the selected video segment, we manually specified the starting and the ending postures of the virtual butterfly, and then use our approach to simulate the rest. In particular, all the maneuvering angles were automatically computed in the simulation process. Finally, we rendered the virtual butterfly into the original video to generate a comparison video. Figure 15 shows a snapshot of the generated comparison video. We can see that during the flight, the



Fig. 15. A virtual butterfly is rendered into a video footage with a real butterfly. The right butterfly is the virtual butterfly while the left one is a real butterfly. For the video result, please refer to the supplemental demo video.

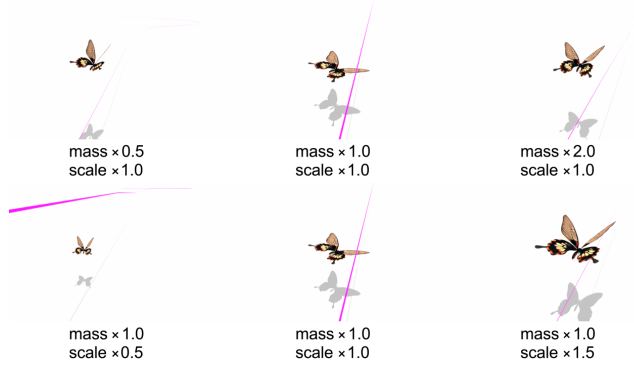


Fig. 16. Comparisons of butterflies with different masses or scales. The top row shows that a simulated butterfly with different masses, while the bottom row shows the virtual butterfly with different scales. Basically, a smaller mass makes the butterfly fly higher due to the lift force, and vice versa. And, a virtual butterfly with larger wings can fly higher and produce more instantaneous vertical oscillations.

wing-abdomen interaction of the virtual butterfly is visually similar to that of the real one. Please refer to the demo video for the comparison result.

Comparisons with different masses. To study the influence of different masses on butterfly flight simulations, we simulated the flights of a virtual butterfly with different masses. During this comparison, we fixed the values of other parameters of a swallow-tail butterfly, except the mass parameter ($x 0.5$, $x 1.0$, and $x 2.0$, respectively). In our approach, the mass can influence the aerodynamics force and thus the acceleration of the butterfly. Also, our simulation results (refer to the top row of Figure 16 and the supplemental demo video) show that, (i) a smaller mass makes the butterfly fly higher due to the lift force, and vice versa; (ii) a larger mass in general makes the butterfly have a higher flapping frequency and amplitude during flights.

Comparisons with different scales. To study the effect of the size of wing area on the flights of simulated butterflies (e.g.,

lift force and drag force), we compared simulated butterflies with different scales. In this comparison, we fixed the values of all other parameters, except the size (scale) of the butterfly model ($x 0.5$, $x 1.0$, and $x 1.5$, respectively). In our model, the wing area can influence both the lift force and the drag force. According to Equation (4), a larger area of the wings will produce larger lift and drag forces. Our simulation results (refer to the bottom row of Figure 16 and the supplemental demo video) also validate this point. Virtual butterflies with larger wings can fly higher and produce more instantaneous vertical oscillations.

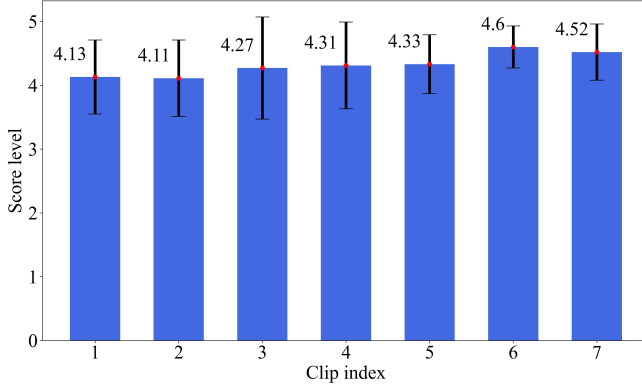


Fig. 17. The average values and the variances of all the 7 stimuli in our user study. The score variances of the 7 stimuli (clip index from 1 to 7) are 0.59, 0.61, 0.75, 0.60, 0.47, 0.34, and 0.44, respectively. The clip index 1 denotes the “flying along a user-specified path” simulation; clip index 2 denotes the “interacting with wind” simulation; clip index 3 denotes the “flying in the rain” simulation; clip index 4 denotes the “chasing” simulation; clip index 5 denotes the “aggregation” simulation; clip index 6 denotes the “traveling” simulation; and the clip index 7 denotes the “direct comparison with a real butterfly” simulation. More details of the 7 stimuli are described in Table 4.

7.3 User Studies

To qualitatively evaluate the simulation results by our approach, we conducted user studies using a 5-point Likert scale. A total of 152 participants, arranged as two groups, were recruited to participate in our user studies. The first group (called *Group One*) has 107 participants (12 females and 95 males; from 20 to 40 years old), and the second group (called *Group Two*) has 45 participants (16 females and 29 males; from 20 to 37 years old). Most of them are university students in the fields of engineering and computer science, knowing little about computer animation or artistic design.

Realism user study. A total of 7 simulation results (described in Table 4), with ID from 1 to 7, were used as the stimuli in the realism study. All the 107 participants in the “Group One” participated in this study. Each participant can watch each stimulus unlimited times before giving his/her rating, and before the start of the experiment the participants were informed that the minimum score 1 denotes “not realistic at all”, and the maximum score 5 denotes “super realistic - just like real butterflies”. The results of the realism study are illustrated in Figure 17, where both the average values and the variances of the obtained scores for all the stimuli are reported.

Table 5. The average values, variances, and statistical test results of the user scores obtained in the validation user study. “Baseline” in the EXPER column refers to the “comparison with a baseline approach” experiment (in Section 7.2). In the Baseline row, “BL” in the method column denotes the baseline approach and “ours” denotes our method. “Ablation” in the EXPER column refers to the “Ablation study” experiment. In the ablation row, “w/o VF” denotes our method without vortex force, and “ours” denotes our complete method.

EXPER	method	scores		F-ratio	p-value
		Average	Variance		
Baseline	BL	2.02	0.57	260.6	<0.01
	ours	4.49	0.48		
Ablation	w/o VF	1.93	0.56	297.9	<0.01
	ours	4.44	0.39		

As shown in this figure, the average score of all the stimuli is 4.32. Also, the first and second stimuli (i.e., clip index #1 “flying along a user-specified path” and clip index #2 “interacting with wind”) received lower scores than the other stimuli. Arguably, the main reason is that, in the first two simulations, the butterfly was rendered without any background environment (that is, a pure white background), which may affect the participants’ visual perception on the butterfly. By contrast, the #6 and #7 stimuli, which denote the swam “traveling” simulation and the “direct comparison with a real butterfly” simulation respectively, received high average scores and low variances. This realism study validates that our approach can generate realistic butterfly flight motion in various real-world settings.

To analyze the reliability of the received user ratings in the above realism study, we use the Cronbach’s alpha (α^c) as a coefficient to test the internal consistency. It can be computed as follows:

$$\alpha^c = \left(\frac{n}{n-1} \right) \left(\frac{\sigma^2 - \sum \sigma_i^2}{\sigma^2} \right), \quad (13)$$

where σ^2 denotes the total variance, n is the total number of the used stimuli, and σ_i^2 denotes the score variance of the i -th stimulus. The score variances of all the 7 stimuli are shown in Figure 17. The computed total variance is 11.61. The computed Cronbach’s alpha α^c is 0.78. Note that $\alpha^c > 0.7$ is generally considered as an acceptable threshold for internal consistency.

In addition, after the studies, we asked the participants to send us their free-form opinions on “what is the main visual difference between a simulated butterfly and a real one.” We received a total of 15 responses, most of which point out that the main visual difference is the subtle softness and weaving motion effect on the butterfly wings’ surface. This shows there is still room for further improving the visual realism of simulated butterfly flights.

Validation user study. We also conducted a validation user study to evaluate the 2 simulation results from the baseline comparison experiment (Section 7.2) and the 2 simulation results from the ablation study experiment (Section 7.2). All the 45 participants in the “Group Two” participated in this study. Just like in the above realism study, participants were asked to give a score from 1 (not

realistic at all) to 5 (just like real butterflies) for each watched simulation. As shown in Table 5, our method received a higher average score than the baseline method, and the scores of the ablation study clips indicate that the introduced vortex force in our model helps to produce more realistic butterfly flight motion. We used the ANOVA method to compute the p-values for the two comparisons (reported in Table 5). The computed *p*-values of the two comparisons are smaller than 0.01, which means there are statistically significant differences between the two stimuli in each of the comparison pairs, that is, between the baseline method and our method, and between the ablation study version (without vortex force) and our complete approach.

8 DISCUSSION AND CONCLUSION

In this paper we present a practical approach to efficiently simulate butterfly flights in various real-world settings. Specifically, we introduce a force-based model, including a simplified aerodynamics force and a vortex force, to animate the fast undulating of wing-abdomen interaction during butterfly flights. We also introduce motion decoupling into the maneuvering control of the flying butterfly. Through experiments, comparisons, and user study, we demonstrate that our model can real-time generate realistic butterfly animations for different scenarios.

Despite the demonstrated effectiveness, our current method has several limitations, described below.

- Our current approach can simulate the wing-abdomen interaction of the butterfly. However, it does not include the simulation of butterfly takeoff and landing motions, which may need certain coordination between legs and body. Specifically, based on our observations, insects may obtain momentum from both the wings' flapping and the legs' jumping. Furthermore, the butterfly may not simply apply the lift force to obtain the thrust through the down-stroke during a take-off motion [Johansson and Hennigsson 2021]. This could be different from the normal flight state, where the butterfly obtains the lift force through down-stroke.
- The maneuvering functions in our current approach are mostly inspired by existing biological and bio-mechanical literature. Due to the practical difficulty and challenge of acquiring ground-truth motion (in particular, both the wings and body motion) of butterflies in natural outdoor environments, we are not able to obtain such data for our model calibration or training. Therefore, the simulated motion by our current approach may not be perfectly aligned with real butterflies in the natural world, although it is practical and efficient to generate visually compelling simulations.
- The skeleton-driven body deformation in our current approach is insufficient to produce the subtle softness and weaving motion effects, often observed on the wings of a real butterfly. Advanced deformation and simulation algorithms (e.g., physically-accurate modeling algorithms) need to be designed to achieve such subtle simulations. We also observe that the weaving motion of butterfly wings often propagates from the root to the wing-tip, from the leading-edge to the opposite edge, and from the fore-wings to the hind-wings. Therefore,

to simulate realistic weaving motion effect observed on the butterfly wings, we need to computationally model the relationship between the forces acted on the wings and weaving motion effect.

As the future work, we plan to build an in-house motion acquisition setup to acquire accurate motion of butterflies in indoor settings, and then we will utilize such data to calibrate our model, or develop new data-driven approaches to accurately model and animate virtual butterflies. Also, we plan to develop novel algorithms to simulate the landing and take-off motions of butterflies in virtual environment.

ACKNOWLEDGMENTS

Zhigang Deng was supported in part by US NSF IIS-2005430. Xiaogang Jin was supported in part by the National Natural Science Foundation of China (Grant Nos. 62036010, 61972344), and the Ningbo Major Special Projects of the “Science and Technology Innovation” (Grant No. 2020Z007).

REFERENCES

- CR Betts and RJ Wootton. 1988. Wing shape and flight behaviour in butterflies (Lepidoptera: Papilionoidea and Hesperioidae): a preliminary analysis. *Journal of experimental biology* 138, 1 (1988), 271–288.
- Ayodeji T Bode-Oke and Haibo Dong. 2020. The reverse flight of a monarch butterfly (*Danaus plexippus*) is characterized by a weight-supporting upstroke and postural changes. *Journal of the Royal Society Interface* 17, 167 (2020), 20200268.
- Robert Bridson, Jim Hourihan, and Marcus Nordenstam. 2007. Curl-noise for procedural fluid flow. *ACM Transactions on Graphics (ToG)* 26, 3 (2007), 46–es.
- Qiang Chen, Guoliang Luo, Yang Tong, Xiaogang Jin, and Zhigang Deng. 2019. Shape-constrained flying insects animation. *Computer Animation and Virtual Worlds* 30, 3–4 (2019), e1902.
- Iain D Couzin, Jens Krause, Richard James, Graeme D Ruxton, and Nigel R Franks. 2002. Collective memory and spatial sorting in animal groups. *Journal of theoretical biology* 218, 1 (2002), 1–11.
- William Dickson, Andrew Straw, Christian Poelma, and Michael Dickinson. 2006. An integrative model of insect flight control. In *44th AIAA Aerospace Sciences Meeting and Exhibit*. 34.
- Robert Dudley. 1991. Biomechanics of flight in Neotropical butterflies: aerodynamics and mechanical power requirements. *Journal of Experimental Biology* 159, 1 (1991), 335–357.
- Robert Dudley. 2002. *The biomechanics of insect flight: form, function, evolution*. Princeton University Press.
- Charles Ellington. 1984a. The aerodynamics of hovering insect flight. I. The quasi-steady analysis. *Philosophical Transactions of the Royal Society of London. B, Biological Sciences* 305, 1122 (1984), 1–15.
- Charles Ellington. 1984b. The aerodynamics of hovering insect flight. V. A vortex theory. *Philosophical Transactions of the Royal Society of London. B, Biological Sciences* 305, 1122 (1984), 115–144.
- Hua Huang and Mao Sun. 2012. Forward flight of a model butterfly: Simulation by equations of motion coupled with the Navier-Stokes equations. *Acta Mechanica Sinica* 28, 6 (2012), 1590–1601.
- Yura Hwang, Theodore A Uyeno, and Shinjiro Sueda. 2019. Bioinspired simulation of knotting hagfish. In *International Symposium on Visual Computing*. Springer, 75–86.
- Koji Isogai, Shun Fujishiro, Taku Saitoh, Manabu Yamamoto, Masahide Yamasaki, and Manabu Matsubara. 2004. Unsteady three-dimensional viscous flow simulation of a dragonfly hovering. *AIAA journal* 42, 10 (2004), 2053–2059.
- Benjamin Jantzen and Thomas Eisner. 2008. Hindwings are unnecessary for flight but essential for execution of normal evasive flight in Lepidoptera. *Proceedings of the National Academy of Sciences* 105, 43 (2008), 16636–16640.
- LC Johansson and P Hennigsson. 2021. Butterflies fly using efficient propulsive clap mechanism owing to flexible wings. *Journal of the Royal Society Interface* 18, 174 (2021), 20200854.
- Eunjung Ju, Jungdam Won, Jehee Lee, Byungkuk Choi, Junyong Noh, and Min Gyu Choi. 2013. Data-driven control of flapping flight. *ACM Transactions on Graphics (TOG)* 32, 5 (2013), 1–12.
- Chang-kwon Kang, Jacob Cranford, Madhu K Sridhar, Deepa Kodali, David Brian Landrum, and Nathan Slegers. 2018. Experimental characterization of a butterfly in climbing flight. *AIAA Journal* 56, 1 (2018), 15–24.

- Chengzhe Li, Hua Wang, Xiaoming Chen, Jun Yao, Lei Shi, and Chengli Zhou. 2017. Role of visual and olfactory cues in sex recognition in butterfly *Cethosia cyane*. *Scientific reports* 7, 1 (2017), 1–9.
- Colin R McInnes. 2007. Vortex formation in swarms of interacting particles. *Physical Review E* 75, 3 (2007), 032904.
- Xiangfei Meng, Junjun Pan, Hong Qin, and Pu Ge. 2018. Real-time fish animation generation by monocular camera. *Computers & Graphics* 71 (2018), 55–65.
- Gavin SP Miller. 1988. The motion dynamics of snakes and worms. In *Proceedings of the 15th annual conference on Computer graphics and interactive techniques*. 169–173.
- Steven E Naranjo. 2019. Assessing insect flight behavior in the laboratory: a primer on flight mill methodology and what can be learned. *Annals of the Entomological Society of America* 112, 3 (2019), 182–199.
- Alejandro Ortega Ancel, Rodney Eastwood, Daniel Vogt, Carter Ithier, Michael Smith, Rob Wood, and Mirko Kovač. 2017. Aerodynamic evaluation of wing shape and wing orientation in four butterfly species using numerical simulations and a low-speed wind tunnel, and its implications for the design of flying micro-robots. *Interface focus* 7, 1 (2017), 20160087.
- Ken Perlin. 2002. Improving noise. In *ACM transactions on graphics (TOG)*, Vol. 21. ACM, 681–682.
- Igor V Pivkin, Eduardo Hueso, Rachel Weinstein, David H Laidlaw, Sharon Swartz, and George E Karniadakis. 2005. Simulation and visualization of air flow around bat wings during flight. In *International Conference on Computational Science*. Springer, 689–694.
- Jiapeng Ren, Wanxuan Sun, Dinesh Manocha, Aming Li, and Xiaogang Jin. 2018. Stable information transfer network facilitates the emergence of collective behavior of bird flocks. *Physical Review E* 98, 5 (2018), 052309.
- Craig W Reynolds. 1987. Flocks, herds and schools: A distributed behavioral model. In *Proceedings of the 14th annual conference on Computer graphics and interactive techniques*. 25–34.
- Kei Senda, Takuya Obara, Masahiko Kitamura, Tomomi Nishikata, Norio Hirai, Makoto Iima, and Naoto Yokoyama. 2012. Modeling and emergence of flapping flight of butterfly based on experimental measurements. *Robotics and Autonomous Systems* 60, 5 (2012), 670–678.
- Nathan Slegers, Michael Heilman, Jacob Cranford, Amy Lang, John Yoder, and Maria Laura Habegger. 2017. Beneficial aerodynamic effect of wing scales on the climbing flight of butterflies. *Bioinspiration & biomimetics* 12, 1 (2017), 016013.
- Madhu Sridhar, Chang-Kwon Kang, and D Brian Landrum. 2016. Instantaneous lift and motion characteristics of butterflies in free flight. In *46th AIAA Fluid Dynamics Conference*. 3252.
- Madhu Sridhar, Chang-Kwon Kang, and Taeyoung Lee. 2020. Geometric Formulation for the Dynamics of Monarch Butterfly with the Effects of Abdomen Undulation. In *AIAA Scitech 2020 Forum*. 1962.
- RB Srygley and ALR Thomas. 2002. Unconventional lift-generating mechanisms in free-flying butterflies. *Nature* 420, 6916 (2002), 660–664.
- Finlay J Stewart, Michiyo Kinoshita, and Kentaro Arikawa. 2015. The roles of visual parallax and edge attraction in the foraging behaviour of the butterfly *Papilio xuthus*. *Journal of Experimental Biology* 218, 11 (2015), 1725–1732.
- H. Tanaka and I. Shimoyama. 2010. Forward flight of swallowtail butterfly with simple flapping motion. *Bioinspiration Biomimetics* 5, 2 (2010), 026003.
- Xinjie Wang, Xiaogang Jin, Zhigang Deng, and Linling Zhou. 2014. Inherent noise-aware insect swarm simulation. In *Computer Graphics Forum*, Vol. 33. Wiley Online Library, 51–62.
- Xinjie Wang, Jiaping Ren, Xiaogang Jin, and Dinesh Manocha. 2015. BSSwarm: biologically-plausible dynamics model of insect swarms. *Proceedings of the 14th ACM SIGGRAPH/Eurographics Symposium on Computer Animation* (2015), 111–118.
- Z Jane Wang. 2005. Dissecting insect flight. *Annu. Rev. Fluid Mech.* 37 (2005), 183–210.
- Hong Will. 2020. Dynamic Bone. <https://assetstore.unity.com/packages/tools/animation/dynamic-bone-16743>.
- Tyler Wilson and Roberto Albertani. 2014. Wing-flapping and abdomen actuation optimization for hovering in the butterfly *Idea leuconoe*. In *52nd Aerospace Sciences Meeting*. 0009.
- Jia-chi Wu and Zoran Popović. 2003. Realistic modeling of bird flight animations. *ACM Transactions on Graphics (TOG)* 22, 3 (2003), 888–895.
- Wei Xiang, Jiaping Ren, Kuan Wang, Zhigang Deng, and Xiaogang Jin. 2019. Biologically inspired ant colony simulation. *Computer Animation and Virtual Worlds* 30, 5 (2019), e1867.
- Naoto Yokoyama, Kei Senda, Makoto Iima, and Norio Hirai. 2013. Aerodynamic forces and vortical structures in flapping butterfly's forward flight. *Physics of Fluids* 25, 2 (2013), 4191–4208.
- John Young, Joseph CS Lai, and Charly Germain. 2008. Simulation and parameter variation of flapping-wing motion based on dragonfly hovering. *AIAA Journal* 46, 4 (2008), 918–924.
- Chaojiang Zhu, Kazunobu Muraoka, Takeyuki Kawabata, Can Cao, Tadahiro Fujimoto, and Norishige Chiba. 2006. Real-time animation of bird flight based on aerodynamics. *The Journal of the Society for Art and Science* 5, 1 (2006), 1–10.